Report Number:

2020-05-06

A Virtual 4D CT Scanner

Xiwen Li

4D CT scan is widely used in medical imaging. Images are acquired through phases. In this case, we can track the motion of organs such as heart. However, it also introduces motion artifacts. A lot of research focuses on remove these artifacts. It is difficult to acquire artifact data by a real CT scanner. In this project, we implement a virtual CT machine to simulate the real 4D CT scan. we also conduct experi- ments to check its clinical reality with respect to respiratory and heart motion parameters.

A Virtual 4D CT Scanner

Xiwen Li

Abstract

4D CT scan is widely used in medical imaging. Images are acquired through phases. In this case, we can track the motion of organs such as heart. However, it also introduces motion artifacts. A lot of research focuses on remove these artifacts. It is difficult to acquire artifact data by a real CT scanner. In this project, we implement a virtual CT machine to simulate the real 4D CT scan. we also conduct experiments to check its clinical reality with respect to respiratory and heart motion parameters.

1. Introduction

4D CT scan is a widely used imaging method in organ motion caused by breathing. In this project, we develop a virtual 4D multi-slice CT scanner to simulate functionalities of real 4D CT scan. We use XCAT phantom to simulate human target. XCAT phantom provides voxelized model of patient's anatomy. Our experiments include respiratory and heart motion under different parameters.

2. Related Work

Some papers focus on the mechanism of CT scan. Keall [1] analyzes the mechanism of 4D CT scan. Lewis [2] uses mathematical models to analyze the cause of artifacts of nomral CT. There is also algorithmic research. In this project, we take advantage of 4D XCAT Phantom by Segars [3]. This tool provides virtual patients for medical imaging research. It produces voxelized patient models with respiratory and heart motion for certain amount of time. We use it to produce input and ground truth data in this project. Segars [4] also developed a similar tool based on XCAT phantom.

3. Main Algorithm

We simulate 4D multi-slice helix CT scanner. During scanning period, the table rotates and moves upwards from feet of the patient. During each rotation, the table scans a part of human body by detectors. The entire algorithm is illustrated in 1. All scans are perpendicular with coronal plane. Each scan starts from foot to head. As shown in 1,

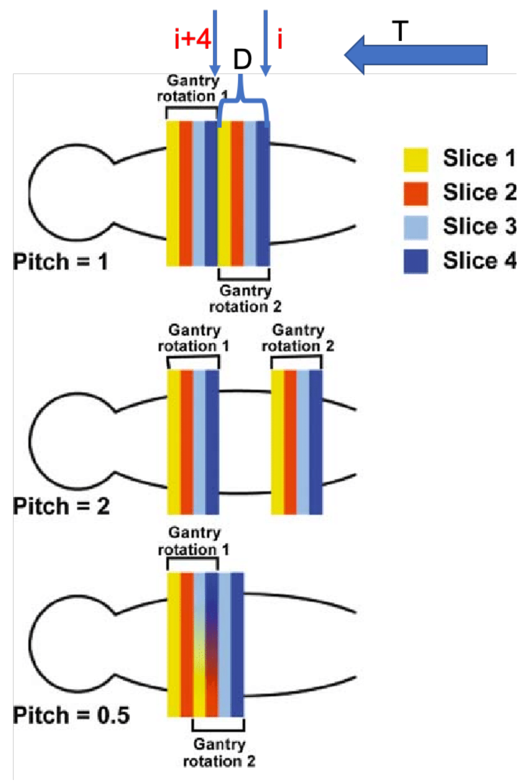

Figure 1. Values of pitch result in three types of scan. Each set of 4 slices represents one scan. Each stripe represents the scan by one detector. Gentry is refered as table.

the table moves by T and scans area with coverage D. Each scan copies corresponding slices from C_f to O_f at position index i. We assume each scan takes 1 second. When table moves to a new position, it holds there for a period of time P to get acquisitions over time. Once it is done, it moves to the next position. We created 200-frame human models. The entire scan is cycled. If the algorithm runs out of 200 frames but the image is not fully reconstructed, the scanner moves back to frame 0 and starts from there.

3.1. Phantom Generation

We generate input phantom collection C. C is also ground truth in our experiments. Each phantom is a 251 x 512 x 512 voxelized cube. The size of each voxel is

Algorithm 1 Virtual Scanner Algorithm

Input: table feed T, detector coverage D, number of slices N, slice spacing s, number of phases P, input phantom collection C, number of frames F, $|C| = F$, time of one rotation r_t
Output: output CT image collection O, $|O| = N$

Initialize real world timer t as $t = 0$
Initialize index $i = 0$ to track table position
Initialize O as the output placehoder
for $i < N$ **do**
  for p in P **do**
    C_f = current phantom at frame f
    C_f^i = current slice at index i
    O_p^i (ith slice on O at frame p) $= C_f^i$
    if $D > T$ **then**
      overwrite previous acquisition
    else if $D < T$ **then**
      $itpl$ = interpolated slices of previous acquisition
      $O_p^{i-(\frac{T}{s}-\frac{D}{s})+1} = itpl$ fill gap
    end if
    $t = t + r_t$
  end for
  $i = i + \frac{T}{s}$ update table position
end for

0.1cm x 0.1cm x 0.1cm. Each C has 200 frames and fps as 10. It is an animated human body model over 20 seconds. Each phantom collection C have both respiratory motion and heart motion.

3.2. Pitch and Data Resampling

In real helix CT scan, the table with detectors scans a certain area by detector coverage $D(mm/s)$ and moves by certain distance $T(mm/s)$. We define $pitch$ as:

$$pitch = \frac{T}{D} \tag{1}$$

When $pitch = 1$, each acquisition is firmly aligned with the end of previous one. Our algorithm does not resample data in this case. When $pitch < 1$, each acquisition scans overlap area with the previous slices. We average the overlap area. When $pitch > 1$, each acquisition has gap between the last one. This is shown in Fig.1. Except the regular acquisition, we fill the gaps with copies of the last slice from previous acquisition.

4. Experiments

4.1. Qualitative Analysis

At first, we check our result visually. Among acquisitions over all phases, we extract slice index at 256 of coronal plane that clearly shows heart shape. As shown in 2, artifact shows up in diaphragm and heart area when $pitch = 1$ and $pitch > 1$. There are obvious shortening, elongation and splitting of shapes.

4.2. Quantitative Analysis

The experiments concentrate on the accuracy of capturing heart motion with respiratory period $resp\_period$, heart beating period hrt_period, maximum diaphragm motion max_d and maximum AP expansion max_{AP}. We use real values. max_d and max_{AP} are combined together. There are three combinations including [0.5, 0.3], [1, 0.6] and [3, 1.8]. $resp\_period$ has 3s, 5s and 7s. hrt_period also has 0.833s, 1s and 1.33s. We conduct two sets of experiments with 27 experiments for each. In set 1, table moves 0.6 mm / s and detector coverage is 0.3 mm / s. Since the table moves more than detector coverage, the scanner interpolates gap area. Results of set 1 is shown in 1. In set 2, we set the table feed to 0.3 mm /s. Its reulst is in 2. The code and data are available at `https://github.com/lix4/CSE598`.

In order to measure the capability of capturing heart motion, we compare union between captured motion $m_a ll$ and the ground truth $t_a ll$ over all frames F. Both of them have 251 x 512 x 512 pixels. We compute the Dice similar coefficient and hausdorff distance of whole heart and left ventricle only. For each set of experiment, we generate 200 frames as our ground truth phantoms. Our 4D CT reconstruction has 10 phases. Results are shown in 3, 4, 1 and 2. 3 shows Dice values of whole heart are generally higher than that of LV. Clinically, tracking of a smaller organ usually has lower accuracy than of a bigger organ. To the same

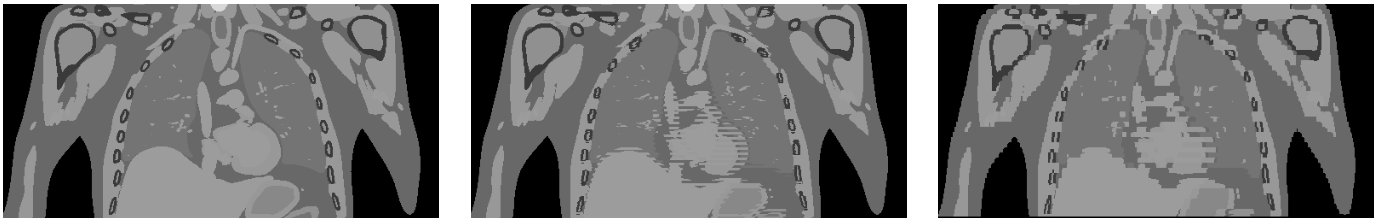

(a) ground truth (b) pitch = 1 (c) pitch > 1

Figure 2. Visual Comparison between Values of Pitch

target, lower pitch value has higher dice value due to interpolation.

5. Conclusion

Using XCAT phantom, our virtual 4D CT scanner can simulate the mechanism of real 4D CT scan. The experiments show our results are consistent with real CT scan visually and statistically. Our scanner is ready to produce 4D CT images for future research.

References

[1] Paul J. Keall, George Starkschall, Himanshu P. Shukla, Kenneth M. Forster, Vivian Ortiz, Craig Stevens, Sastry S. Vedam, Rohini George, Thomas Guerrero, and Ram Mohan. Acquiring 4d thoracic ct scans using a multislice helical method. *Physics in medicine and biology*, 49 10:2053–67, 2004.

[2] John H. Lewis and Steve B. Jiang. A theoretical model for respiratory motion artifacts in free-breathing ct scans. *Physics in medicine and biology*, 54 3:745–55, 2009.

[3] William Segars, G Sturgeon, S Mendonca, Jason Grimes, and Benjamin Tsui. 4d xcat phantom for multimodality imaging research. *Medical physics*, 37:4902–15, 09 2010.

[4] W. P. Segars, M. Mahesh, T. J. Beck, E. C. Frey, and B. M. W. Tsui. Realistic ct simulation using the 4d xcat phantom. *Medical Physics*, 35(8):3800–3808, 2008.

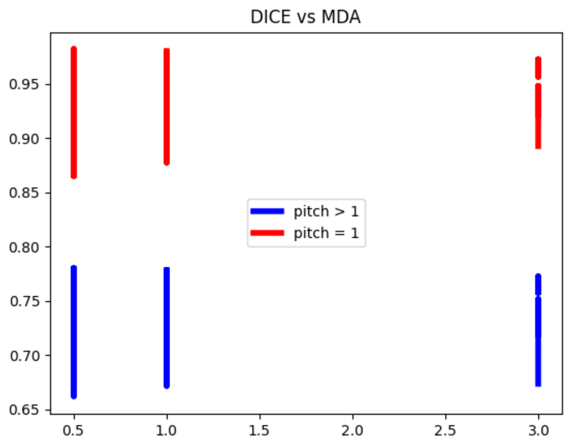

(a)

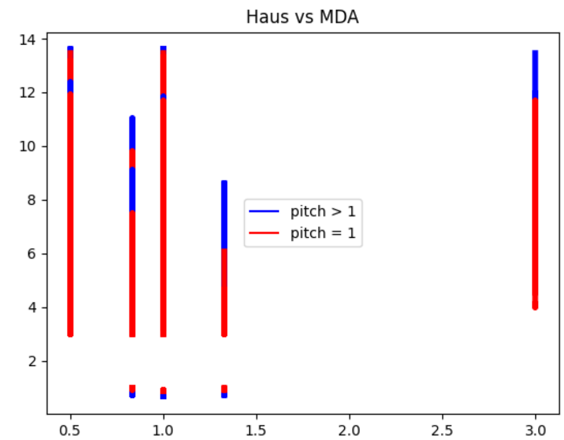

(b)

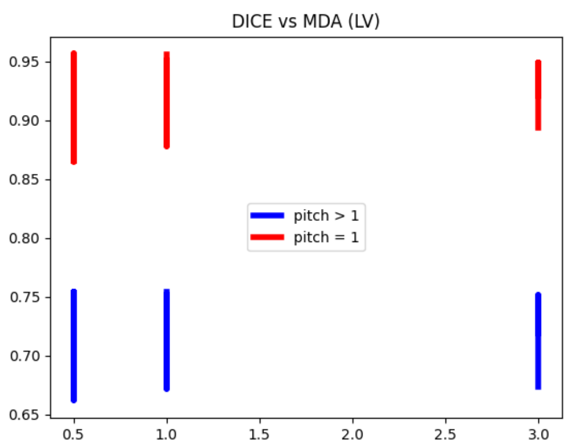

(c)

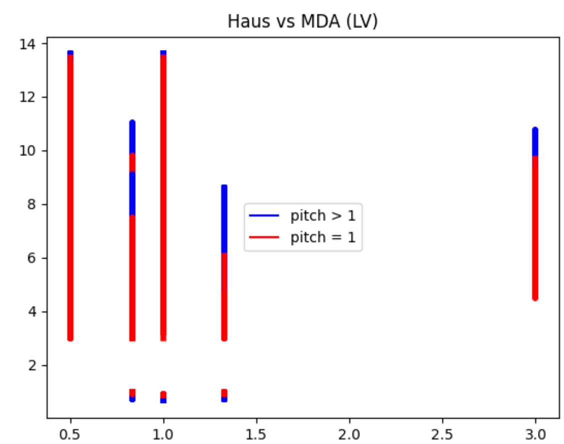

(d)

Figure 3. Comparision between results. (a) Dice values of whole heart with respect to MDA. (b) Haus values of whole heart with respect to MDA. (c) Dice values of LV with respect to MDA. (d) Haus values of LV versus MDA.

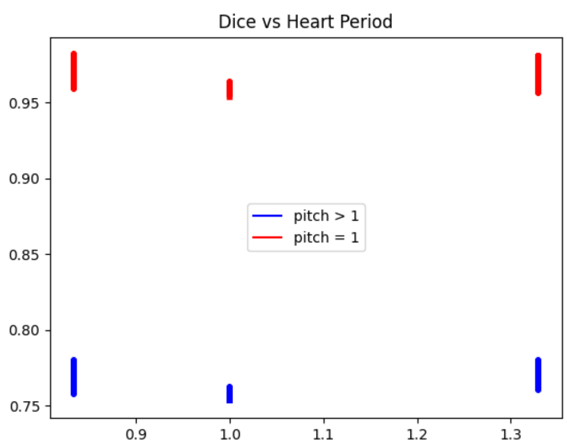

(c)

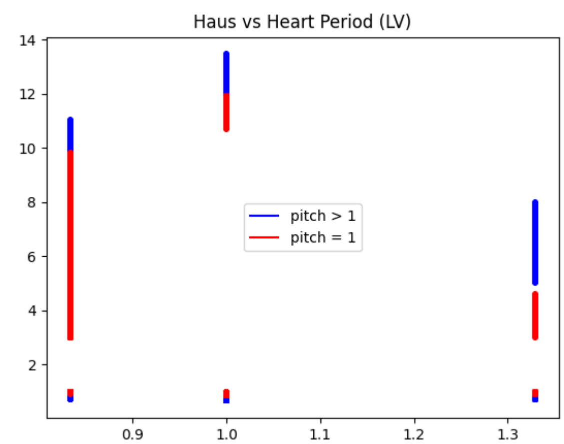

(d)

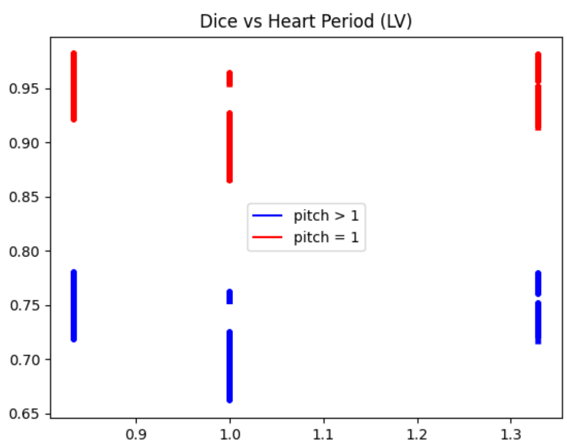

(c)

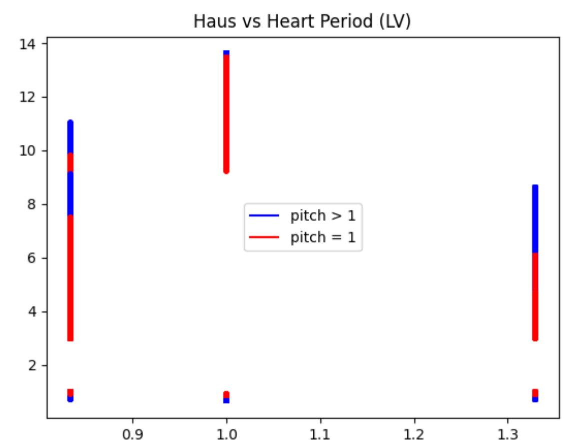

(d)

Figure 4. Comparison between results. (a) Dice values of whole heart with respect to Heart Period (HP). (b) Haus values of whole heart with respect to HP. (c) Dice values of LV with respect to HP. (d) Haus values of LV with respect to HP.

exp	Dice_{whole}	Dice_{LV}	haus_{whole}	haus_{LV}
3, 0.5, 0.3, 0.833	0.779620	0.753659	5.099020	5.000000
5, 0.5, 0.3, 0.833	0.767011	0.726590	6.403124	6.000000
7, 0.5, 0.3, 0.833	0.779977	0.754364	4.123106	4.242641
3, 1.0, 0.6, 0.833	0.778715	0.753808	5.916080	5.000000
5, 1.0, 0.6, 0.833	0.763275	0.720956	7.000000	7.810250
7, 1.0, 0.6, 0.833	0.777927	0.752624	5.744563	5.385165
3, 3.0, 1.8, 0.833	0.771716	0.746114	7.280110	6.000000
5, 3.0, 1.8, 0.833	0.757205	0.718345	11.045361	9.110434
7, 3.0, 1.8, 0.833	0.772340	0.751645	7.874008	7.000000
3, 0.5, 0.3, 1.0	0.753408	0.664392	12.206556	13.601471
5, 0.5, 0.3, 1.0	0.753710	0.661550	12.369317	13.341664
7, 0.5, 0.3, 1.0	0.753170	0.665615	12.000000	13.601471
3, 1.0, 0.6, 1.0	0.754625	0.674784	11.180340	13.076697
5, 1.0, 0.6, 1.0	0.754873	0.671649	11.445523	13.076697
7, 1.0, 0.6, 1.0	0.754105	0.676874	11.832160	13.152946
3, 3.0, 1.8, 1.0	0.758127	0.673164	13.453624	9.797959
5, 3.0, 1.8, 1.0	0.762143	0.724508	12.000000	10.392305
7, 3.0, 1.8, 1.0	0.760474	0.719853	10.816654	10.770330
3, 0.5, 0.3, 1.33	0.778341	0.748692	5.099020	5.000000
5, 0.5, 0.3, 1.33	0.765260	0.720593	7.280110	8.000000
7, 0.5, 0.3, 1.33	0.779705	0.751752	5.000000	4.358899
3, 1.0, 0.6, 1.33	0.777563	0.750544	5.916080	5.385165
5, 1.0, 0.6, 1.33	0.763530	0.716067	7.280110	8.602325
7, 1.0, 0.6, 1.33	0.778368	0.749824	5.196152	4.582576
3, 3.0, 1.8, 1.33	0.770977	0.743924	7.280110	6.000000
5, 3.0, 1.8, 1.33	0.760500	0.729477	8.000000	8.602325
7, 3.0, 1.8, 1.33	0.772459	0.749206	7.348469	7.348469

Table 1. Tracking accuracy of entire heart when $pitch > 1$.

exp	Dice_{whole}	Dice_{LV}	haus_{whole}	haus_{LV}
3, 0.5, 0.3, 0.833	0.982020	0.956288	3.000000	3.000000
5, 0.5, 0.3, 0.833	0.969985	0.931484	5.385165	4.472136
7, 0.5, 0.3, 0.833	0.981560	0.955527	3.162278	3.000000
3, 1.0, 0.6, 0.833	0.980691	0.956189	3.000000	3.000000
5, 1.0, 0.6, 0.833	0.965859	0.924780	6.082763	6.000000
7, 1.0, 0.6, 0.833	0.978537	0.951522	3.605551	3.162278
3, 3.0, 1.8, 0.833	0.973148	0.948444	4.000000	5.656854
5, 3.0, 1.8, 0.833	0.959234	0.920924	9.797959	7.483315
7, 3.0, 1.8, 0.833	0.971561	0.948434	7.874008	4.582576
3, 0.5, 0.3, 1.0	0.955482	0.865697	11.789826	13.453624
5, 0.5, 0.3, 1.0	0.955481	0.864863	11.916375	13.190906
7, 0.5, 0.3, 1.0	0.953872	0.867616	11.916375	13.152946
3, 1.0, 0.6, 1.0	0.958475	0.880563	11.704700	13.341664
5, 1.0, 0.6, 1.0	0.958006	0.877397	11.357817	13.076697
7, 1.0, 0.6, 1.0	0.955555	0.881793	11.045361	13.076697
3, 3.0, 1.8, 1.0	0.962825	0.893214	11.180340	9.695360
5, 3.0, 1.8, 1.0	0.964070	0.926791	11.704700	9.219544
7, 3.0, 1.8, 1.0	0.960718	0.922616	10.677078	9.273618
3, 0.5, 0.3, 1.33	0.980715	0.951165	3.000000	3.000000
5, 0.5, 0.3, 1.33	0.963597	0.915944	3.162278	3.000000
7, 0.5, 0.3, 1.33	0.981146	0.951832	3.162278	3.162278
3, 1.0, 0.6, 1.33	0.979488	0.950773	3.162278	4.000000
5, 1.0, 0.6, 1.33	0.961493	0.913533	4.000000	4.123106
7, 1.0, 0.6, 1.33	0.979293	0.950417	3.162278	3.000000
3, 3.0, 1.8, 1.33	0.972331	0.945749	4.123106	6.082763
5, 3.0, 1.8, 1.33	0.956192	0.919944	4.000000	4.472136
7, 3.0, 1.8, 1.33	0.972338	0.948490	4.582576	4.690416

Table 2. Tracking accuracy of entire heart when $pitch = 1$